A New Local Sine Transform without Overlaps: A Combination of Computational Harmonic Analysis and PDE

Naoki Saito and Jean-François Remy

Department of Mathematics, University of California, Davis, CA 95616 USA

ABSTRACT

We introduce a new local sine transform that can completely localize image information in both the space and spatial frequency domains. Instead of constructing a basis, we first segment an image into local pieces using the characteristic functions, then decompose each piece into two components: the *polyharmonic component* and the *residual*. The polyharmonic component is obtained by solving the elliptic boundary value problem associated with the so-called polyharmonic equation (e.g., Laplace equation, biharmonic equation, etc.) given the boundary values (the pixel values along the borders created by the characteristic functions) possibly with the estimates of normal derivatives at the boundaries. Once this component is obtained, this is subtracted from the original local piece to obtain the residual, whose Fourier sine series expansion has quickly decaying coefficients since the boundary values of the residual (possibly with their normal derivatives) vanish. Using this transform, we can distinguish *intrinsic* singularities in the data from the artificial discontinuities created by the local windowing. We will demonstrate the superior performance of this new transform in terms of image compression to some of the conventional methods such as JPEG/DCT and the lapped orthogonal transform using actual examples.

Keywords: Polyharmonic equation, Laplace equation, local sine transform, singularities and discontinuities, image compression, quantization

1. INTRODUCTION

For smooth periodic signals and images, the conventional Fourier series expansion can give us almost everything we need. Simply manipulating the Fourier coefficients, we can shift them, differentiate/integrate them, and filter/attenuate them at our disposal. We can also measure the smoothness class (the Lipschitz/Hölder exponents) of a signal by checking the rate of the decay of its Fourier coefficients, which is related to sparsity since the faster decay of the expansion coefficients leads to a sparser representation. See the standard references on Fourier series[1–3] for the details. *It is amazing to realize that we lose everything once we have to deal with non-periodic signals.* The mismatch caused by brute-force periodization (i.e., the head and the tail of an input signal do not match) kills every nice property we would have in the case of the smooth periodic signals. Dealing with non-periodic signals in a proper manner is of paramount importance in many applications that require analysis of local signal features such as data compression and discrimination. First of all, real signals are often non-periodic. Second, even if the original signal is perfectly periodic, its locally segmented pieces (for local analysis of such pieces) are almost always not periodic. Thus, what we must do is not to create artificial discontinuities due to the local windowing or brute-force periodization so that we can focus on the analysis of *intrinsic* discontinuities and singularities in the signal if any. Our goal is to develop a transform that can eliminate the interference of the boundary of a local window imposed by a user with the Fourier analysis of the information inside of such a window as much as possible.

We note that the wavelets/wavelet packets do not really solve this problem because in order to use wavelets or wavelet packets one needs to follow one of the following recipes: 1) periodize a signal and apply the standard wavelets/wavelet packets; or 2) design special wavelets near the boundaries (called "the wavelets on interval") as Cohen, Daubechies, and Vial proposed in Ref. 4; or 3) use the so-called "multiwavelets" developed by Alpert,[5] which use the segmented orthogonal polynomials. Unfortunately, none of them is really satisfactory for the applications we are interested in. The brute-force periodization (1) again creates the mismatch/discontinuity at the end points, and this generates large wavelet/wavelet packet coefficients. The wavelets on interval (2) are too

Further author information: E-mail: saito@math.ucdavis.edu; WWW: http://math.ucdavis.edu/~saito

complicated in practice, particularly if one wants to use these in the wavelet packet mode or for images. Finally, the multiwavelets (3) are unfortunately not efficient for oscillatory signals such as textured images.

Coifman and Meyer[6] and Malvar[7,8] independently developed the so-called lapped orthogonal transform (LOT) (also known as local trigonometric transform (LTT) or Malvar wavelets) in an attempt to solve the above problems. However, it turned out that they were not completely satisfactory either, particularly for local signal analysis. The primary reason is the lack of the true localization capability of LTT. LTT cannot split an input signal into a set of non-overlapping (disjoint) regions without the influence of their adjacent regions due to its use of the folding operations. (We will call this a "crosstalk" problem.) In this respect, the block discrete cosine transform (DCT) used in the old JPEG is better because it chops a signal with the characteristic functions, i.e., no influence from the adjacent regions. Chopping the signal with the characteristic functions, however, makes the representation of the signal segment less sparse due to the sharp cutoff at the boundaries of the segment. In the case of LTT, we can tune the width of the overlap in the folding operations, but there is another dilemma. The wider the overlap, the better in terms of sparsity, but the worse in terms of crosstalks (i.e., more statistically dependent). Fang and Séré developed the so-called "multiple folding" local trigonometric transforms (MLTT)[9] to overcome one of the problems. In terms of sparsity, MLTT provides a better representation than the conventional LTT. However, in terms of crosstalk problems, MLTT is definitely worse than LTT because MLTT has wider overlaps, especially in the early stage of the hierarchical split, and that creates more and more crosstalks down in the hierarchy.

All these problems essentially boil down to how to treat the boundaries that define those subintervals and regions. To attack this fundamental problem, we recently developed a new version of the local Fourier transform called "continuous boundary local Fourier transform" (CBLFT) that does not create any crosstalks among the subintervals and any discontinuities in the signal values at the boundaries of those subintervals.[10,11] Briefly speaking, CBLFT first chops a signal into segments with the characteristic functions. Let $I = [0, 1]$ be one of the segment for simplicity. Then, the segmented signal on I, say, $f(x)$ is periodized. Let us assume that f is continuous on I. Consider now the interval of length $3|I|$, i.e., $[-1, 2]$. At this point, the head and tail of f on I does not match, so the periodized signal has two discontinuities at $x = 0$ and $x = 1$. Now, we add the constant $f(0) - f(1)$ to this periodized signal only over $[-1, 0]$, and similarly $f(1) - f(0)$ only over $[1, 2]$. This makes this extended signal continuous over $[-1, 2]$ although this is not periodic anymore. CBLFT then applies the folding operations at $x = 0$ and $x = 1$ and follows the usual LFT recipe of Wickerhauser.[12,13] This procedure guarantees the decay of $O(k^{-2})$ where k is the frequency index, generates no crosstalks since it only uses the signal information over I, and moreover, allows us to use the complex exponentials instead of real-valued cosine functions, which may be advantageous for certain applications such as computing locally analytic signals. However, CBLFT is still not completely satisfactory in terms of sparsity. It does not deal with discontinuities in the derivatives of an input signal so that the speed of the decay of the expansion coefficients is not fast enough. Moreover, due to its use of the folding operators, CBLFT is not too effective for very short segments of a signal.

We will propose the *Polyharmonic Local Sine Transform* (PHLST) in the next section, which is a fundamentally better transform in the sense that it does not suffer from any of these problems compared to the other methods mentioned above. It can also easily and hierarchically be generalized to a higher dimension. The PHLST paradigm belongs to a larger class of models, which Yves Meyer refers to as the $u + v$ models.[14] In a $u + v$ model, data $f(x)$ are assumed to be a sum of two components $u(x)$ and $v(x)$. The first component $u(x)$ is aimed at modeling the objects present in the data whereas the $v(x)$ term is responsible for texture and noise in the data. One can also interpret $u(x)$ as "trend" and $v(x)$ as "fluctuation" of a signal, which are commonly-used terms in the wavelet literature.[15] In our PHLST paradigm, we specifically use the solution of the *polyharmonic equation* (e.g., the Laplace or biharmonic equations) given the boundary condition which imposes that the u component exactly matches the original data at the region boundaries. This u component, however, becomes very smooth away from the boundaries and only carry the low frequency information in the middle of the region. The *residual* $v(x) = f(x) - u(x)$, therefore, have less boundary effect and retains the original texture information almost intact. Because the v component vanishes at the boundaries, this component is suitable for *Fourier sine series expansion* since the magnitudes of the expansion coefficients decay quickly, i.e., $O(k^{-3})$ or faster.

The organization of this paper is as follows. We will describe the basic idea of PHLST in the next section as well as important practical information, in particular, implementation issues. Section 3 reports the results of

our simple compression experiments using DCT, local cosine transform (LCT; one version of LTT), and PHLST. The results are very promising for PHLST. Finally, we conclude this paper by Section 4 where we discuss our future plans and relation of PHLST to the previous works done by other scientists.

2. OUR PROPOSED METHOD: POLYHARMONIC LOCAL SINE TRANSFORM

Instead of constructing a basis, we first segment a signal $f(\boldsymbol{x})$, $\boldsymbol{x} \in \mathbb{R}^d$ into local pieces using the characteristic functions, then split each piece into two components: the polyharmonic component and the residual. Let $\Omega \in \mathbb{R}^d$ be the overall domain where the signal is supported, and let $\overline{\Omega} = \cup_{j=1}^J \overline{\Omega}_j$ be a decomposition of the domain Ω into a set of disjoint subdomains $\{\Omega_j\}$. Note that Ω_j's are open and disjoint whereas $\overline{\Omega}_j$'s are closed and may share the boundaries. Let f_j be the restriction of f to Ω_j and let us consider the $u+v$ model locally on Ω_j, i.e., $f_j = u_j + v_j$. We call u_j the *polyharmonic component* of f_j and v_j the *residual*. Let Δ be the Laplace operator in $\mathbb{R}^d$. Then the polyharmonic component is obtained by solving the following polyharmonic equation:

$$\Delta^m u_j = 0 \quad \text{in } \Omega_j, \quad m = 1, 2, \ldots \tag{1}$$

with given boundary values and normal derivatives

$$\frac{\partial^{p_\ell} u_j}{\partial n^{p_\ell}} = \frac{\partial^{p_\ell} f}{\partial n^{p_\ell}} \quad \text{on } \partial\Omega_j, \quad \ell = 0, \ldots, m-1, \tag{2}$$

where p_ℓ is the order of the normal derivatives to be specified. The parameter p_0 must always be set to 0, which means that $u_j = f$ on the boundary $\partial\Omega_j$. These boundary conditions enforce the signal values and normal derivatives of orders $p_1, \ldots, p_{m-1}$ of the solution u_j along the boundary $\partial\Omega_j$ to match those of the original signal f over there. If the Ω_j's are all rectangles (of possibly different sizes), then we take $p_\ell = 2\ell$, i.e., the *even order* normal derivatives. It is not necessary to match the odd order normal derivatives if we expand v_j into the Fourier sine series because it is equivalent to the Fourier series expansion of the extension of v_j by odd reflection with respect to the boundary $\partial\Omega_j$ and the continuity of the odd order normal derivatives is automatic. Note that in practice the normal derivatives need to be estimated using the available sample values of f. See Section 4.1 for more about this issue of estimation. For $m = 1$, Equation (1) is of the form:

$$\begin{aligned} \Delta u_j &= 0 \quad \text{in } \Omega_j, \\ u_j &= f \quad \text{on } \partial\Omega_j, \end{aligned} \tag{3}$$

which is the *Laplace equation with Dirichlet boundary condition.* For $m = 2$, we have the following *biharmonic equation with the mixed boundary condition*:

$$\begin{aligned} \Delta^2 u_j &= 0 \quad \text{in } \Omega_j, \\ u_j = f, \quad \frac{\partial^\ell u_j}{\partial n^\ell} &= \frac{\partial^\ell f}{\partial n^\ell} \quad \text{on } \partial\Omega_j, \end{aligned} \tag{4}$$

where $\ell = 1$ or 2 depending on the shape of Ω_j. For the rectangular-shaped Ω_j, we take $\ell = 2$. Note that in 1D ($d = 1$), the solution of (3) is simply a linear function connecting two boundary points of an interval $\overline{\Omega}_j$ whereas that of (4) is a cubic polynomial. However, in higher dimension, the solutions of (3), (4), and more generally (1) with (2) are not a tensor product of algebraic polynomials in general.

Subtracting such $u_j(\boldsymbol{x})$ from $f_j(\boldsymbol{x})$ gives us the residual $v_j(\boldsymbol{x}) = f_j(\boldsymbol{x}) - u_j(\boldsymbol{x})$ satisfying:

$$\frac{\partial^{p_\ell} v_j}{\partial n^{p_\ell}} = 0 \quad \text{on } \partial\Omega_j, \quad \ell = 0, \ldots, m-1. \tag{5}$$

Since the values and normal derivatives of v_j on $\partial\Omega_j$ vanish, its Fourier sine expansion coefficients decay rapidly, i.e., $O(\|\boldsymbol{k}\|^{-2m-1})$, if there is no other intrinsic singularity in Ω_j. In fact, we have the following theorem.

Theorem 2.1. *Let Ω_j be a bounded rectangular domain in $\mathbb{R}^d$, and let $f_j \in C^{2m}(\overline{\Omega}_j)$, but non-periodic. Assume further that $(\partial/\partial x_i)^{2m+1} f$, $i = 1, \ldots, d$, exist and are of bounded variation. Furthermore, let $f_j = u_j + v_j$ be the PHLST representation, i.e., the polyharmonic component u_j is the solution of the polyharmonic equation (1) of order m with the boundary condition (2) with $p_\ell = 2\ell$, $\ell = 0, 1, \ldots, m-1$, and $v_j = f_j - u_j$ is the residual component. Then, the Fourier sine coefficient $b_{\boldsymbol{k}}$ of the residual v_j is of $O\left(\|\boldsymbol{k}\|^{-2m-1}\right)$ for all $\boldsymbol{k} \neq \boldsymbol{0}$, where $\boldsymbol{k} = (k_1, \ldots, k_d) \in \mathbb{Z}_+^d$, and $\|\boldsymbol{k}\|$ is the usual Euclidean (i.e., ℓ^2) norm of $\boldsymbol{k}$.*

The proof of this theorem can be found in our longer version of this paper.[16] Note that if we employ the straightforward Fourier series expansion of non-periodic f_j by brute-force periodization, the decay rate is only $O\left(\|\boldsymbol{k}\|^{-1}\right)$ even if $f_j \in C^{2m}(\overline{\Omega}_j)$. If we use the Fourier cosine series expansion, we can get $O\left(\|\boldsymbol{k}\|^{-2}\right)$.

We call this new way of decomposing a function f into a set of functions $\{f_j = u_j + v_j\}_{j=1}^{J}$ the *Polyharmonic Local Sine Transform* (PHLST) with polyharmonicity m. For $m = 1$ and 2, we use the special abbreviations, LLST (Laplace LST) and BLST (Biharmonic LST).

Remark 2.2. The polyharmonic component is smooth particularly in the middle of the region Ω_j and as $\boldsymbol{x}$ approaches the boundary $\partial\Omega_j$, u_j approaches f. In fact, u_j is also the minimizer of the following optimization problem (see e.g., Ref. 17):

$$\min_{u \in H^m(\Omega_j)} \sum_{|\alpha|=m} \binom{m}{\alpha} \int_{\Omega_j} |D^\alpha u|^2 \mathrm{d}\boldsymbol{x} \quad \text{subject to the boundary condition (2)}, \tag{6}$$

where $H^m(\Omega_j)$ is a Sobolev space of order m over Ω_j, $\alpha = (\alpha_1, \cdots, \alpha_d)$ is a multi-index of an d-dimensional variable with the following definitions: $|\alpha| = \alpha_1 + \cdots + \alpha_d$, $\binom{m}{\alpha} = m!/(\alpha_1! \cdots \alpha_d!)$, and $D^\alpha = \partial_1^{\alpha_1} \cdots \partial_d^{\alpha_d}$, where $\partial_i = \partial/\partial x_i$. This means that the polyharmonic component minimizes the *roughness* measured by the objective function in (6) while satisfying the boundary condition (2). The larger the polyharmonicity m is, the smoother the solution u_j gets.

Remark 2.3. Because the u_j component becomes very smooth away from the boundaries and only carry the low frequency information in the middle of the region as discussed in Remark 2.2, the frequency content of the v_j component is close to that of f_j, particularly, around the mid to higher frequency band, where textures are well represented. Therefore, the v_j component retains the original texture information almost intact and is more suitable for texture analysis than the original image f_j.

Remark 2.4. Another interpretation of this decomposition $f_j = u_j + v_j$ is the following: the polyharmonic component u_j represents the part of f_j that is *predictable using the boundary information only*, whereas the residual v_j represents the *unpredictable* part of f_j. Yet another interpretation of this decomposition is that the u_j and v_j components represent the *trend* and *fluctuation* of f_j, respectively.

If Ω and Ω_j's are rectangular regions in $\mathbb{R}^d$, which is the most practical case in terms of numerical implementation, we can employ the Discrete Sine Transform (DST) based on the FFT algorithm to rapidly compute both the polyharmonic components and the Fourier sine series expansion of the residual components. In particular, we use the algorithm proposed by Averbuch, Braverman, Israeli, and Vozovoi,[18,19] which seems to us the most natural and practical Laplace/Poisson equation solver on rectangles. This ABIV method gives us more accurate solutions than those based on the finite difference (FD) approximation of the Laplace operator followed by FFT,[20,21] which only gives solutions with accuracy $O(h^2)$ and $O(h^4)$ for the so-called 5-point and modified 9-point FD approximations, respectively (h is, of course, the grid spacing here). Yet, the computational cost of the ABIV algorithm is $O(N^d \log N)$ where N is the number of grid points in each direction of a rectangular domain. We also note that we use the $(d-1)$-dimensional version of PHLST to represent and compress the boundary function $f(\boldsymbol{x})$ for $\boldsymbol{x} \in \partial\Omega_j$.

Let us show a simple example of the effect of removing the polyharmonic component. Figure 1 demonstrates this. Here, we only used the global version of LLST, i.e., no further split of the image and the u component is the solution of the Laplace equation. One may wonder what is the difference between the original and the residual v component in this case because they look very similar. We would like to point out that the v component is displayed in a shifted dynamic range (i.e., $[-127, 127]$ instead of $[0, 255]$) to see the details. Moreover, if we examine them carefully, we can observe that the overall shading is gone in the residual. The bottom row of Figure 1 clarifies this by displaying them as 3D perspective plots.

Figure 2 shows the results of LLST decomposition by splitting the original into a set of homogeneous rectangular regions each of which has 17×17 pixels.

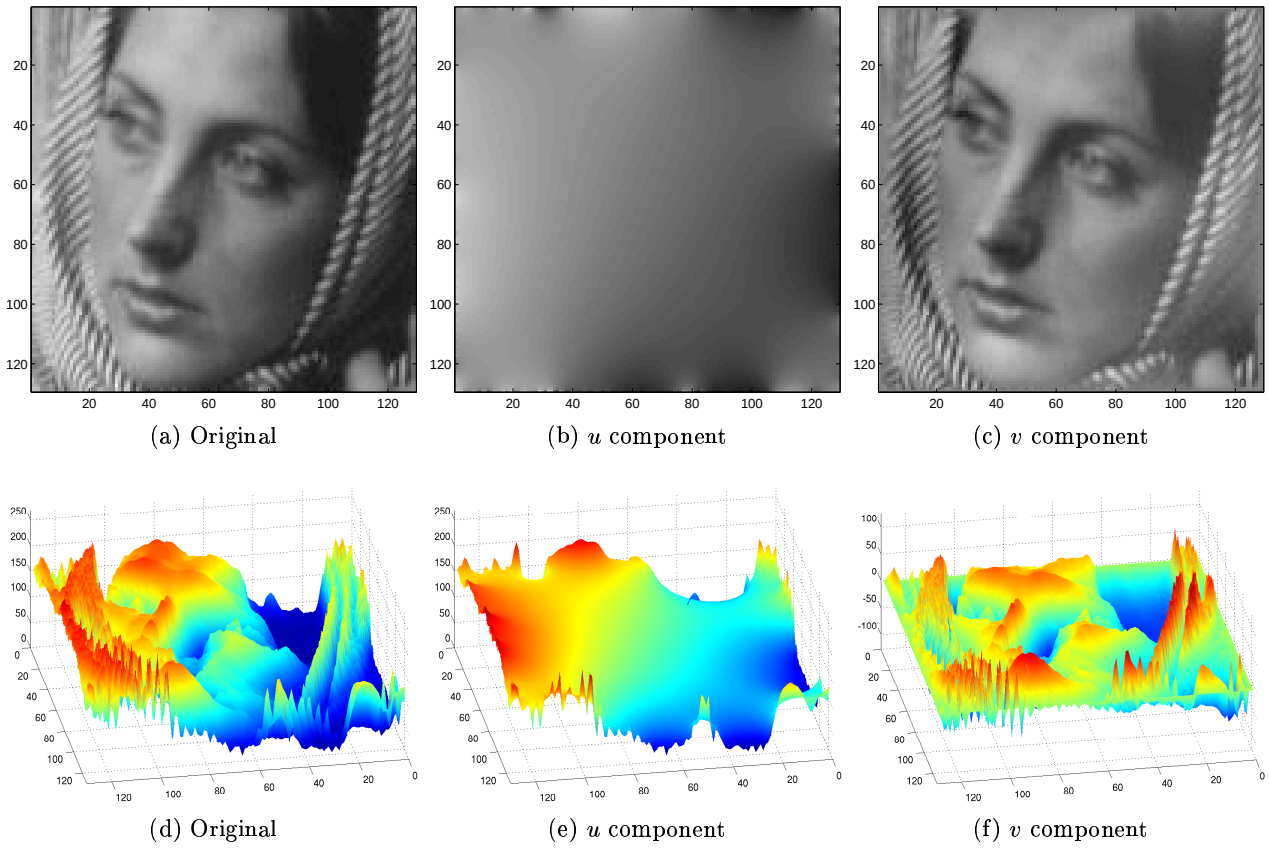

(a) Original (b) u component (c) v component

(d) Original (e) u component (f) v component

Figure 1. The global version of LLST applied to the face part (129×129 pixels) of the Barbara image. Note that the display dynamic range of (a) and (b) are set to $[0, 255]$ whereas that of (c) is set to $[-127, 127]$. Figures (d)–(f) are the 3D perspective plots of the top row. It is easier to see in (f) that the overall shading of the face is removed in the residual component v.

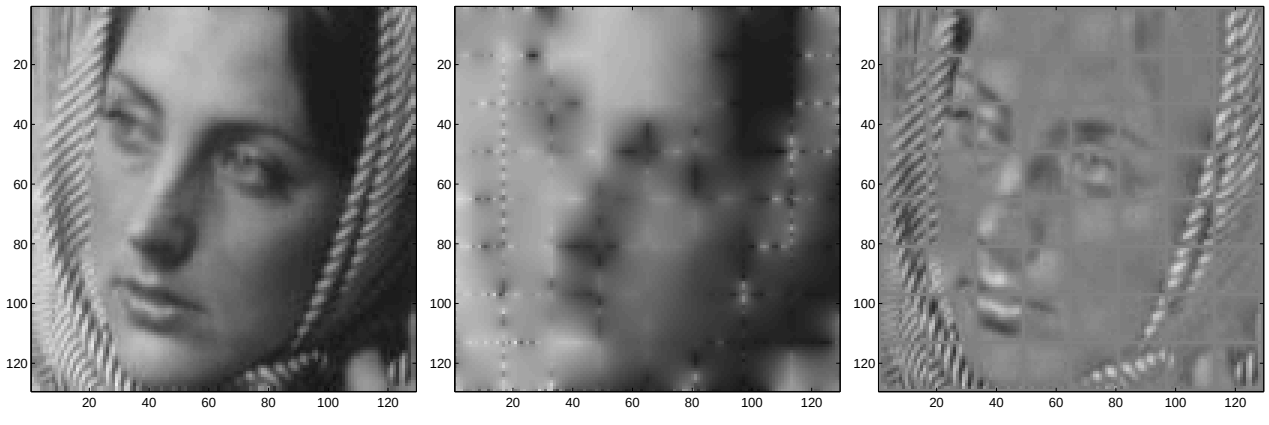

(a) Original (b) $\cup_j u_j$ (c) $\cup_j v_j$

Figure 2. The hierarchical LLST decomposition of the Barbara face image. The middle image represents $\cup_j u_j$ where each Ω_j is a square of 17×17 pixels. The right image represents $\cup_j v_j$.

3. COMPRESSION EXPERIMENTS

Using LLST, we conducted a simple image compression experiment and compared the results with DCT and LCT, including the quantization process. We note that our experiment presented here is of limited nature: 1) we only used one image; 2) we only used the homogeneous partition of an input image into 16×16 pixel blocks for DCT/LCT and 17×17 pixel blocks for LLST; 3) we only used a particular quantization method called *matrix quantization*; 4) we only compared the performance of LLST with that of DCT and LCT; 5) we only used the standard orthonormal bell[13] for LCT and the width of the bell is fixed throughout the hierarchy (see Ref. 22 for more extensive compression tests of LCT with different bells); 6) we only performed LLST (i.e., $m = 1$), not the higher order PHLST; 7) we only used the same compression rate (0.4 bits/pixel) for all cases; 8) we used the same compression rate for compressing both the residual components and the boundary values for LLST although it was possible to use different rates. Recall that the boundary values are also transformed by the 1D version of LLST before compression. Much larger and more thorough experiments are currently being conducted and the results will be reported at a later date.

Let us now explain a little bit more about the JPEG-DCT and its quantization. In the lossy JPEG standard, an input image is split into a set of homogeneous blocks of 8×8 pixels, and the 2D DCT coefficients of each block are computed. Then, these coefficients in each block are arithmetically divided by a matrix called Quantization Matrix (QM) in the element-wise fashion, then rounded to the nearest integers.[23] The elements of QM corresponding to the higher frequency coefficients have larger values than those for the lower frequency coefficients so that this quantization process can result in many zeros (i.e., more compression) without sacrificing visual fidelity too much. To decompress the compressed representation, the QM is multiplied first and then the inverse 2D DCT is applied. Although the JPEG standard allows us to use a user-specified QM, the standard QM most often used in practice is the one determined by psychophysical experiments on the visibility of the DCT basis vectors.[23] This standard QM is optimized for DCT of 8×8 pixel blocks, but optimal for neither DCT of blocks of different sizes nor DST of blocks of any size. Therefore, we need to calibrate the QM specifically for DST used in PHLST. Our intern, David Nicault, conducted small scale psychophysical experiments (using 11 subjects) to determine the best QM of size 9×9 for PHLST.[24] In our compression experiments, we used 16×16 pixel blocks for DCT/LCT and 17×17 pixel blocks for PHLST. In order to create the QMs of these sizes, we employed a very simple (suboptimal) approach: we duplicated the rows and columns of the QMs for all three cases. We would like to note that Nicault did test psychophysically for the QM of 17×17 pixel blocks. However, he only got one subject for this test instead of 11 due to the time constraint. Therefore, we decided to postpone the use of this optimized QM for 17×17 until we conduct more psychophysical experiments although the preliminary results suggest that this optimized QM performs better than the one with column/row duplication used in this paper.

We note that in the 1D LLST representation of each boundary segment, the u component can be reduced to just two numbers (slope and y-intercept), and the DST coefficients of the v component is quantized by the first column or row of the QM of size 17×17. The 1D version of the QM for boundaries should also be determined through the psychophysical experiments. In fact, Nicault conducted such experiments,[24] but due to the same reason as above (insufficient subjects), we again decided to postpone its use. In our experiments below, the compression rates and entropy values of course include both boundary and inside information for LLST.

Figure 3 shows the results of our experiments. To see the details, Figure 4 shows the zoomed-up versions of the decompressed images around the left eye region. We also computed the PSNR values for each case. PSNR (peak signal-to-noise ratio)—a better metric for image quality than SNR—is defined as $20 \log_{10}(\max_{\boldsymbol{x} \in \Omega} |f(\boldsymbol{x})|/RMSE)$ where $RMSE$ (the root mean square error) is the absolute ℓ^2 error between the original and reconstruction divided by the square root of the number of pixels.

Our results suggest that LLST is very promising for image compression. In terms of PSNR, LLST was essentially the same as DCT and better than LCT. Moreover, the annoying blocking effect apparent in DCT was suppressed in LLST. This version of LCT also revealed the crosstalk problem all over the place and resulted in a less sharp reconstruction than those of DCT and LLST. On the other hand, this version of LLST is not yet optimal due to the use of the fixed size blocks. The smooth regions such as the forehead in this image should be bounded by larger blocks to gain more compression. This suggests that adaptive segmentation based on the smoothness of the region will be critical for the further success for LLST. More about this in Section 4.2.

(a) Original (b) DCT

(c) LCT (d) LLST

Figure 3. Compression of the face part of the Barbara image by DCT, LCT, and LLST. The image was divided into a set of homogeneous blocks of size 16×16 pixels for DCT/LCT and 17×17 for LLST. The entropy of compressed representation is 0.4 bits/pixel (bpp) for each case, i.e., compression rate of 20. Their PSNR values (in dB) are 29.55, 28.42, and 29.54, respectively.

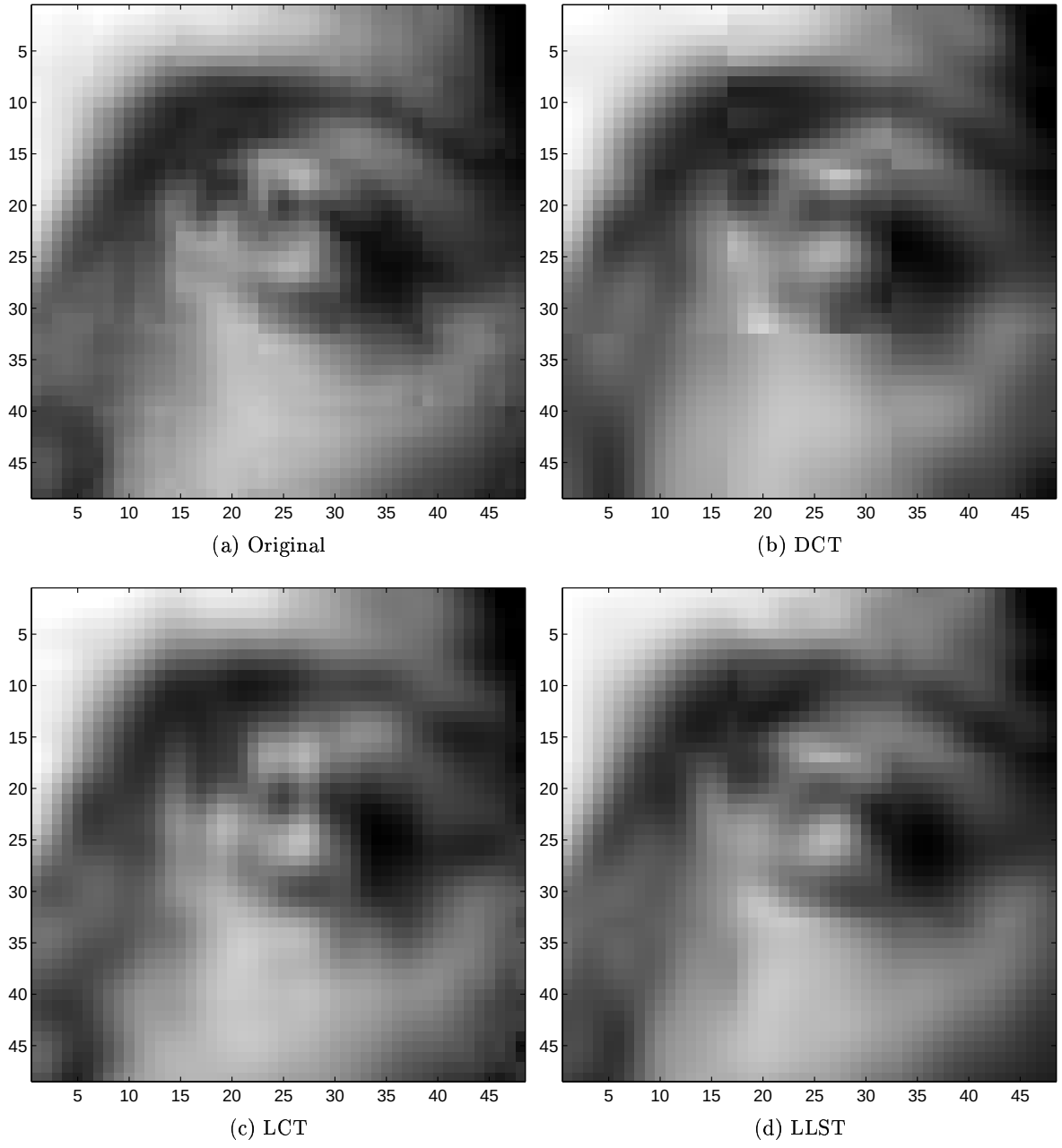

(a) Original (b) DCT

(c) LCT (d) LLST

Figure 4. Zoomed up versions of Figure 3.

4. DISCUSSION

4.1. Dealing with Noise

Since our PHLST relies so much on the given boundary values, one may wonder what happens if the boundary values are noisy. We are currently investigating the effect of noise on the boundary (as well as in the interior) of a given domain. In particular, if we want to use the higher precision version of the ABIV Laplace equation solver, we need to estimate the even order derivatives on the boundary. We expect that it is difficult to estimate the derivatives of order beyond 2 even without noise. In this paper, we only used the actual boundary values, not the second derivatives. However, it is very interesting to check whether we can improve our compression quality using the higher precision Laplace equation solver using second derivative estimates at the corners of each block. Also, BLST will need second derivative estimates not only at the corners but also at all the boundary points. Currently, we are conducting experiments using the parabola fitting and the method of Lanczos[25] for estimating the second derivatives. The parabola fitting, however, is very sensitive to noise. Therefore, the method of Lanczos will be our choice. We will report our investigation into the issue of noise and our denoising strategy using PHLST at a later date.

4.2. How to Select the Optimal Segmentation?

We are also investigating several approaches to approximate image segmentation that follows structures of input data, e.g., edges and textured regions. In particular, we are investigating a hierarchical and recursive split-and-merge strategy similar to the best-basis algorithm. Clearly, the key is what criterion we should employ to judge whether smaller blocks should be merged into larger blocks. One of the most promising criteria is the *Minimum Description Length* (MDL) criterion.[26–29] Viewing a split pattern of an image into a set of blocks and a decomposition of a function f_j on block Ω_j into u_j and v_j components as a *model*, the MDL criterion suggests that we should choose among many possible models the one giving the shortest description (counted in bits) of the data *and* the model, which leads to the minimization of the infidelity of the model to the data and the complexity of the model itself in a balanced manner. In the case of PHLST, the MDL criterion is particularly appealing since PHLST does not provide a "basis", so the sparsity criterion using ℓ^p norm with $0 < p \leq 1$ makes less sense contrary to the local cosine dictionary case, for example. It makes more sense to count the description length in bits needed to encode both the boundary values for the polyharmonic component u_j and the DST coefficients of the residual v_j. Again, the encoding of a boundary function should be based on modeling it by the 1D version of PHLST. Another advantage of MDL is to allow us to incorporate various noise models and prior models for distribution of the expansion coefficients, i.e., it can select the most suitable noise model and coefficient distribution models out of many competing models. This is advantageous since it is well known that the Laplacian distribution is more suitable to model natural images than the Gaussian distribution (see e.g., Ref. 30). We plan to report our results at a later date.

4.3. Potential Applications of PHLST

Because of its ability to completely localize the analysis of an input image and sparsify its representation equipped with a fast algorithm, there are many potential applications of PHLST. For example, its application to image zooming and interpolation is very promising since PHLST does not have a boundary effect, which is often a nuisance in image zooming. Commonly used image zooming/interpolation techniques such as pixel replication, bilinear interpolation, bi-cubic interpolation have all drawbacks. Pixel replication is computationally very fast, but generates very annoying blocky zoomed images, especially for large magnification. Bilinear interpolation generates superfluous horizontal and vertical artifacts especially for large magnification, and this is also true for bi-cubic interpolation to a lesser extent. One can use DCT for image zooming, but again one can see the artifacts generated by the even reflection at the boundaries. Sinc (or band-limited) interpolation is theoretically ideal but its straightforward implementation does not work due to the Gibbs phenomenon.

Another important application of PHLST is local feature computation. PHLST allows us to evaluate and compute various attributes (e.g., directional derivatives) at *any point* of the domain Ω_j even if we start from a discrete digital image. We are currently investigating how to get interpolated values of an image along a given *curve* as well as directional derivatives along such a curve, which is not easy using the conventional methods.

Also, as Figure 1 suggests, PHLST may be used to remove shading from an image, which may be particularly important for computing Principal Components of images since shading dominates first several eigenvectors due to its huge amount of energy.

The simple, hierarchical, and recursive algorithmic structure of PHLST will be also useful to implement the higher dimensional version of PHLST, in particular, 3D.

4.4. Relation to the other work

Retrospectively speaking, our work is related to many previous works done by other scientists. However, we did not find exactly the same strategy as ours in the other works. As early as 1938, Cornelius Lanczos[31] suggested that "denoising" and interpolation of digital signals sampled on a *equispaced* grid over a *finite interval* should be very nicely dealt with by trigonometric polynomials once the edge effect is taken care of. This was only an abstract given at AMS conference. Somehow, a full version of the paper did not appear until 1952.[32] He first used the line removal idea[31] corresponding to the 1D LLST in our case, and then proposed to remove a higher order polynomials.[25,32] As far as we know, Lanczos is one of the first scientists who recognized the importance of representing and interpolating data sampled at equispaced grid points using a combination of trigonometric polynomials and algebraic polynomials. He clearly understood that only using algebraic polynomials leads to the infamous Runge phenomenon, and only using trigonometric polynomial leads to the Gibbs phenomenon. Zygmund had a similar idea (i.e., removal of singularities) for different purposes in 1935 or earlier.[33] See also Refs. 2, 34, 35, and 25. Also, the book of Kantrovich and V. I. Krylov[36] cites an early attempt of extending a function supported on $[0,1]$ to $[-1,1]$ smoothly and periodically (with period 2) by Maliev.[37,38] Smirnov[39] also cites the work of A. N. Krylov for speeding up the decay of Fourier coefficients of a compactly supported function using the line and polynomial removal.

In 1990, Madych and Nelson[40,41] introduced the so-called "polyharmonic cardinal splines", which uses the polyharmonic equations to interpolate the data given on the lattice $\mathbb{Z}^d$ in $\mathbb{R}^d$. Their main concern, however, is the interpolation, and they are not concerned with the residuals at all.

The "polysplines" proposed by Kounchev[42,43] are also related to our PHLST. In his case, though, he used a sequence of decreasing subdomains $\Omega = \Omega_0 \supset \Omega_1 \supset \cdots$ instead of the disjoint subdomains of our case. This lead him to develop a new version of multidimensional wavelets. Again, he is not concerned with the residuals.

All of the above scientists except Lanczos only focused on the u component. As far as we know, Lanczos was the only one who seriously considered the residual v, but explored his idea neither for higher dimensions nor for multiscale setting.

ACKNOWLEDGMENTS

This research was partially supported by the ONR grant N00014-00-1-0469. We thank Prof. Gregory Beylkin at University of Colorado, Boulder for fruitful discussions on numerical issues of the Laplace equation solvers. We also thank David Nicault for his work optimizing the quantization matrix for DST/PHLST, which will be reported separately at a later date.

REFERENCES

1. G. H. Hardy and W. W. Rogosinski, *Fourier Series*, Cambridge Univ. Press, third ed., 1956. Republished by Dover Publications, Inc. in 1999.
2. A. Zygmund, *Trigonometric Series*, Cambridge Mathematical Library, Cambridge Univ. Press, third ed., 2003. Volumes I & II combined.
3. M. A. Pinsky, *Introduction to Fourier Analysis and Wavelets*, Brooks/Cole, 2002.
4. A. Cohen, I. Daubechies, and P. Vial, "Wavelets on the interval and fast wavelet transforms," *Appl. Comput. Harmonic Anal.* **1**, pp. 54–81, Dec. 1993.
5. B. K. Alpert, "A class of bases in L^2 for the sparse representation of integral operators," *SIAM J. Math. Anal.* **24**(1), pp. 246–262, 1993.

6. R. R. Coifman and Y. Meyer, "Remarques sur l'analyse de Fourier à fenêtre," *Comptes Rendus Acad. Sci. Paris, Série I* **312**, pp. 259–261, 1991.
7. H. S. Malvar, "The LOT: transform coding without blocking effects," *IEEE Trans. Acoust., Speech, Signal Process.* **37**, pp. 553–559, 1989.
8. H. S. Malvar, "Lapped transforms for efficient transform/subband coding," *IEEE Trans. Acoust., Speech, Signal Process.* **38**, pp. 969–978, 1990.
9. X. Fang and E. Séré, "Adapted multiple folding local trigonometric transforms and wavelet packets," *Appl. Comput. Harmonic Anal.* **1**, pp. 169–179, 1994.
10. B. Larson and N. Saito, "The continuous boundary local Fourier transform," in *Wavelets IX*, A. F. Laine, M. A. Unser, and A. Aldroubi, eds., **Proc. SPIE 4478**, pp. 415–426, 2001.
11. B. Larson, *The Continuous Boundary Local Trigonometric Transform.* PhD thesis, Dept. Math., Univ. California, Davis, 2002.
12. M. V. Wickerhauser, "Smooth localized orthonormal bases," *Comptes Rendus Acad. Sci. Paris, Série I* **316**, pp. 423–427, 1993.
13. M. V. Wickerhauser, *Adapted Wavelet Analysis from Theory to Software*, A K Peters, Ltd., Wellesley, MA, 1994. with diskette.
14. Y. Meyer, *Oscillating Patterns in Image Processing and Nonlinear Evolution Equations*, vol. 22 of *University Lecture Series*, AMS, Providence, RI, 2001.
15. S. Jaffard, Y. Meyer, and R. D. Ryan, *Wavelets: Tools for Science & Technology*, SIAM, Philadelphia, PA, 2001.
16. N. Saito and J.-F. Remy, "The polyharmonic local sine transform: A new tool for local image analysis and synthesis without edge effect," tech. rep., Dept. Math., Univ. California, Davis, 2003.
17. G. Wahba, *Spline Models for Observational Data*, vol. 59 of *CBMS-NSF Regional Conference Series in Applied Mathematics*, SIAM, Philadelphia, 1990.
18. A. Averbuch, M. Israeli, and L. Vozovoi, "A fast Poisson solver of arbitrary order accuracy in rectangular regions," *SIAM J. Sci. Comput.* **19**(3), pp. 933–952, 1998.
19. E. Braverman, M. Israeli, A. Averbuch, and L. Vozovoi, "A fast 3D Poisson solver of arbitrary order accuracy," *J. Comput. Phys.* **144**, pp. 109–136, 1998.
20. W. L. Briggs and V. E. Henson, *The DFT: An Owner's Manual for the Discrete Fourier Transform*, SIAM, Philadelphia, PA, 1995.
21. A. Iserles, *A First Course in the Numerical Analysis of Differential Equations*, Cambridge Texts in Applied Mathematics, Cambridge Univ. Press, New York, 1996.
22. F. G. Meyer, "Image compression with adaptive local cosines: A comparative study," *IEEE Trans. Image Process.* **11**(6), pp. 616–629, 2002.
23. W. B. Pennebaker and J. L. Mitchell, *JPEG Still Image Data Compression Standard*, Van Nostrand Reinhold, New York, 1993.
24. D. Nicault, "Image processing–basis perception study," tech. rep., Dept. Math., Univ. California, Davis, June 2003. UC Davis-Ecole Polytechnique Internship Report.
25. C. Lanczos, *Discourse on Fourier Series*, Hafner Publishing Co., New York, 1966.
26. J. Rissanen, *Stochastic Complexity in Statistical Inquiry*, World Scientific, Singapore, 1989.
27. M. H. Hansen and B. Yu, "Model selection and the principle of minimum description length," *J. Amer. Statist. Assoc.* **96**(454), pp. 746–774, 2001.
28. Y. G. Leclerc, "Constructing simple stable descriptions for image partitioning," *Intern. J. Computer Vision* **3**, pp. 73–102, 1989.
29. N. Saito, "Simultaneous noise suppression and signal compression using a library of orthonormal bases and the minimum description length criterion," in *Wavelets in Geophysics*, E. Foufoula-Georgiou and P. Kumar, eds., ch. XI, pp. 299–324, Academic Press, San Diego, CA, 1994.
30. M. Hansen and B. Yu, "Wavelet thresholding via MDL: simultaneous denoising and compression," *IEEE Trans. Inform. Theory* **46**(5), pp. 1778–1788, 2000.
31. C. Lanczos, "A simple interpolation method for the representation of rugged curves." Abstract of contributed paper given at the November Meeting of the AMS in Cleveland, OH, Nov. 25–26, 1938.

32. C. Lanczos, "Smoothing of noisy data by trigonometric truncation," in *National Bureau of Standards Report*, (1582), pp. 1–16, 1952.
33. A. Zygmund, *Trigonometrical Series*, Chelsea Publishing Co., 1952.
34. C. Lanczos, *Applied Analysis*, Prentice-Hall, Inc., Englewood Cliffs, NJ, 1956. Republished by Dover Publications, Inc. in 1988.
35. C. Lanczos, *Linear Differential Operators*, D. Van Nostrand Co., New York, 1961. Republished by Dover Publications, Inc. in 1997.
36. L. V. Kantrovich and V. I. Krylov, *Approximate Methods of Higher Analysis*, Interscience Publishers, Inc., New York, 1958.
37. A. S. Maliev, "Fourier series of heightened convergence for functions defined in a given interval," *Izv. AN SSSR OMEN* **10**, pp. 1437–1450, 1932.
38. A. S. Maliev, "On the expansion in Fourier series of heightened convergence of functions defined in a given interval," *Izv. AN SSSR OMEN* **8**, pp. 1113–1120, 1933. (Russian).
39. V. I. Smirnov, *A Course of Higher Mathematics*, vol. II, Pergamon Press, New York, 1964. Translated by D. E. Brown.
40. W. R. Madych and S. A. Nelson, "Polyharmonic cardinal splines," *J. Approx. Theory* **60**(2), pp. 141–156, 1990.
41. W. R. Madych and S. A. Nelson, "Polyharmonic cardinal splines: A minimization property," *J. Approx. Theory* **63**(3), pp. 303–320, 1990.
42. O. I. Kounchev, "Minimizing the Laplacian of a function squared with prescribed values on interior boundaries–theory of polysplines," *Trans. Amer. Math. Soc.* **350**(5), pp. 2105–2128, 1998.
43. O. Kounchev, *Multivariate Polysplines: Applications to Numerical and Wavelet Analysis*, Academic Press, San Diego, CA, 2001.